A comparative study of folate receptor-targeted doxorubicin delivery systems: Dosing regimens and therapeutic index

A comparative study of folate receptor-targeted doxorubicin delivery systems: Dosing regimens and therapeutic index

Anna Scomparin[1], Stefano Salmaso[2], Anat Eldar-Boock[1], Dikla Ben-Shushan[1], Shiran Ferber[1], GaliaTiram[1], Hilary Shmeeda[3], Natalie Landa-Rouben[4], Jonathan Leor[4], Paolo Caliceti[2], Alberto Gabizon[3] and Ronit Satchi-Fainaro[1]*

[1]Department of Physiology and Pharmacology, Sackler School of Medicine, Room 607,

[2]Department of Pharmaceutical and Pharmacological Sciences, University of Padova, Via F. Marzolo 5, Padova 35131, Italy.

[3]Department of Oncology, Shaare Zedek Medical Center and Hebrew University-School of Medicine, POB 3235, 91031 Jerusalem, Israel.

[4]Neufeld Cardiac Research Institute, Sheba Medical Center, Tel-Aviv University, Tel-Hashomer, Israel

Running Title: Folate receptor-targeted nanomedicines for cancer therapy

Key Words: Angiogenesis, polymer therapeutics, pullulan, liposomes, doxorubicin, folate receptor targeting.

***Corresponding Author:**

Ronit Satchi-Fainaro, Ph.D., Department of Physiology and Pharmacology, Sackler School of Medicine, Tel Aviv University, Israel.

Tel: +972-3-640 7427; Fax: +972-3-640 9113;

E-mail: ronitsf@post.tau.ac.il

doi: 10.1016/j.jconrel.2015.04.009.

ABSTRACT

Ligand-receptor mediated targeting may affect differently the performance of supramolecular drug carriers depending on the nature of the nanocarrier. In this study, we compare the selectivity, safety and activity of doxorubicin (Dox) entrapped in liposomes *versus* Dox conjugated to polymeric nanocarriers in the presence or absence of a folic acid (FA)-targeting ligand to cancer cells that overexpress the folate receptor (FR). Two pullulan (Pull)-based conjugates of Dox were synthesized, (FA-PEG)-Pull-(Cyst-Dox) and (NH_2-PEG)-Pull-(Cyst-Dox). The other delivery systems are Dox loaded PEGylated liposomes (PLD, Doxil®) and the FR-targeted version (PLD-FA) obtained by ligand post-insertion into the commercial formulation. Both receptor-targeted drug delivery systems (DDS) were shown to interact *in vitro* specifically with cells via the folate ligand.

Treatment of FR-overexpressing human cervical carcinoma KB tumor-bearing mice with three-weekly injections resulted in slightly enhanced anticancer activity of PLD-FA compared to PLD and no activity for both pullulan-based conjugates. When the DDS were administered intravenously every other day, the folated-Pull conjugate and the non-folated-Pull conjugate displayed similar and low antitumor activity as free Dox. At this dosing regimen, the liposome-based formulations displayed enhanced antitumor activity with an advantage to the non-folated liposome. However, both liposomal formulations suffered from toxicity that was reversible following treatment discontinuation. Using a daily dosing schedule, with higher cumulative dose, the folated-Pull conjugate strongly inhibited tumor growth while free Dox was toxic at this regimen. For polymeric constructs, increasing dose intensity and cumulative dose strongly affects the therapeutic index and reveals a major therapeutic advantage for the FR-targeted formulation. All DDS were able to abrogate doxorubicin-induced cardiotoxicity. This study constitutes the first side-by-side comparison of two receptor-targeted ligand-bearing systems, polymer therapeutics *versus* nanoparticulate systems, evaluated in the same mouse tumor model at several dosing regimens.

INTRODUCTION

For more than a century, since Paul Ehrlich established the "magic bullet" concept [1], generations of chemists and pharmacologists have attempted to devise powerful and specific anticancer drugs, that go directly to their intended targets yet remain harmless to healthy tissues. Despite groundbreaking achievements, most anticancer drugs suffer from narrow therapeutic window and cancer still threatens numerous lives owing to its multi-dimensional complexity. In recent years, different versatile macromolecular systems, commonly defined as nanomedicines, have been designed and developed for cancer therapy [2, 3]. Nano-sized carriers can improve the physico-chemical properties of low molecular weight drugs enhancing their therapeutic index by altering their pharmacokinetics and increasing their accumulation in the target tissue exploiting the enhanced permeability and retention (EPR) effect [4, 5]. However, this non-selective blood circulation and extravasation-dependent targeted strategy, relying solely on the leaky vasculature of tumors is limited due to the heterogeneity of the angiogenic vasculature characterizing different tumor types [6]. Therefore, conjugation of targeting ligands to nanocarriers might overcome the limitations of non-selective delivery to the tumor site, achieving enhanced tumor selectivity and intracellular uptake.

Drug delivery systems (DDS) include supramolecular assemblies for the (i) physical entrapment of drugs, such as liposomes [7, 8] and nanoparticles [9, 10] and (ii) chemical covalent binding of drugs, such as polymer conjugates [11, 12], polymeric micelles [13, 14] and polymersomes [15, 16], named polymer therapeutics [17].

Liposomal formulations have proven to be among the most successful approaches of drug delivery translated to the clinic. These spheroidal phospholipidic vesicles represent a versatile carrier for both hydrophilic and hydrophobic drugs. Due to the simple production, efficient drug loading and ease of tailoring of their physico-chemical and bio-pharmaceutical properties, several liposomal formulations for drug delivery have been developed [18]. Nevertheless, the early liposomal formulations were affected by major uptake by the reticuloendothelial system (RES), which dramatically reduced the circulation half-life [19]. Efforts made to avoid clearance by the immune system [20], resulted in the development of long-circulating (“stealth”) liposomal formulations with the ability of escaping the RES clearance. The most effective approach is the coating of the vesicles surface with poly(ethylene glycol) (PEG) [21], which provides steric hindrance, avoidance of opsonization and thus, guarantees a prolonged circulation in the bloodstream. These features led to the approval of several liposomal formulations for clinical use [22].

Doxil® is a PEGylated liposomal doxorubicin (PLD) formulation approved for the treatment of breast cancer, ovarian cancer, multiple myeloma, and Kaposi’s Sarcoma [22, 23]. PLD accumulates in cancer tissue via non-selective targeting extravasating through the leaky tumor vasculature (EPR effect). Following accumulation in the target tissue, the liposomes undergo degradation leading to the release of the entrapped doxorubicin

(Dox), which is then internalized in the cancer cells as free drug [22]. The advantage of the liposomal formulation compared to free Dox is the reduced cardiac toxicity, while the main adverse effect is the hand-foot syndrome (palmar-plantar erythrodysesthesia), that causes redness, swelling, and pain on the palms of the hands and the soles of the feet. Another toxicity related to PLD is a pseudo-allergic reaction that might appear after the first infusion [22, 24].

In parallel, several polymer therapeutics have been developed for the delivery of Dox [25-27]. A few of them have reached clinical trials [28-30], however, none of them have yet received approval by the main authorities, the US Food and Drug Administration (FDA) and the European Medicines Agency (EMA).

On the basis of Ringsdorf's polymeric carrier concept [31, 32], we recently developed a conjugate of Dox using pullulan as the polymeric backbone [33]. Pullulan is a natural, non-ionic and linear homopolysaccharide formed by repeating units of maltotriose [34]. It has been used in the formulation of several drug delivery systems [35-38], due to its biodegradability, low immunogenicity, reduced toxicity and its fair solubility in aqueous and a few organic solvents [39]. Furthermore, pullulan bears functional groups along the polymer backbone that allow multivalent derivatization with a variety of pendant functions [40].

Pullulan polymers at the nano scale exploit the leaky tumor vasculature and EPR effect to selectively accumulate in cancer tissue [37, 41]. Several pullulan-based delivery systems for anticancer drugs have been developed. These include self-assembling hydrophobized pullulan [42], pH-sensitive pullulan nanoparticles [41] and bioconjugates [37, 43-45] for the delivery of Dox, camptothecin, paclitaxel, alendronate, cisplatin, metothrexate and combretastatin A4. Here, we conjugated Dox to the pullulan backbone via an acid sensitive hydrazone bond, which is stable at physiological pH, but hydrolyzes under acidic conditions, such as those found in endosomes or an even lower pH in lysosomes. The bioconjugate was endowed with targeting properties by introducing folate functions in the supramolecular structure.

In order to confer cellular targeting properties to DDS, many targeting agents have been evaluated [46-50]. Folic acid (FA) is an attractive targeting agent to a large number of cancer cell types that overexpress the folate receptor (FR). This small molecule lacks immunogenicity and can be easily conjugated to supramolecular and macromolecular structures. FR-targeted precision nanomedicines can be exploited for the treatment of cancers and other difficult-to-treat diseases overexpressing folate receptor, such as polycystic kidney disease [51], and inflammatory diseases (e.g. adjuvant arthritis) targeting activated macrophages [52]. Thus, folic acid has been widely used for conjugation to DDS [22]. Aimed at evaluating the targeting properties of FA, we conjugated it both to a doxorubicin-loaded liposome (via ligand post insertion) [53] and to a Dox-pullulan conjugate. Previous studies showed that Dox loaded folated liposomes and Dox conjugated folated pullulan have suitable biopharmaceutical behaviours that make them promising for improved therapeutic performance as compared to the non-

folated counterparts. However, in view of exploiting these novel drug delivery systems for an efficient and targeted cancer treatment, *in vitro* and *in vivo* comparative studies were undertaken to compare the biopharmaceutical and therapeutic performance of the liposomal *vs* polymeric systems. The comparative studies were performed according to advanced and validated *in vitro* and *in vivo* protocols, which could provide some elucidation the influence of the architecture on the DDS behaviour in terms of efficacy and safety. The effect of the supramolecular structures on the antitumor and anti-angiogenic activity and on the targeting properties conferred by the bound FA was investigated testing Dox-equivalent doses in human cancer cell line and on endothelial cells as well as *in vivo* on tumor-bearing mice.

MATERIALS AND METHODS

Materials

Doxorubicin hydrochloride was purchased from Iffect Chemphar Co., LTD. (Shenzhen, P.R. China). Doxil® was supplied by Johnson & Johnson (New Jersey, USA). [^{3}H]-Folic acid (FA) sodium salt was bought from American Radiolabeled Chemicals, Inc. (St. Louis, MO, USA). 3,3'-N-(ε-maleimidocaproic acid)-hydrazidetrifluoroacetic acid salt (EMCH) was obtained from Molecular Biosciences, Inc. (Boulder, CO, USA). Diaminopolyethylene glycol ($PEG_{1900}(NH_2)_2$), ~100 kDa pullulan (Mw/Mn 2.03), folic acid (FA), cholesterol, sodium borohydride ($NaBH_4$), N-hydroxysuccinimide (NHS), N,N'-dicyclohexylcarbodiimide (DCC), and all the solvents were purchased from Fluka (Buchs, Switzerland). Cysteamine (Cyst), 5,5'-dithiobis-(2-nitrobenzoic acid) (DTNB), mannitol, sodium cyanoborohydride ($NaCNBH_3$), 2,4,6-trinitrobenzenesulfonic acid (TNBS),, triscarboxyethylphosphine (TCEP), dithiothreitol (DTT), masson trichrome, and pullulan standard set for gel permeation analyses were obtained from Sigma Chemical Co. (St. Louis, MO,USA). Hydrogenated soybean phosphatidyl-choline (HSPC) was purchased from Lipoid, (Duisburg, Germany). Distearoyl-phosphatidylethanolamine conjugated to 2 kDa monomethoxy-poly(ethylene glycol) ($mPEG_{2000}$-DSPE) was obtained from Bio-lab (Jerusalem, Israel). Folate derivatized $mPEG_{3350}$-DSPE (FA-PEG_{3350}-DSPE) was supplied by Shaare Zedek Experimental Oncology Lab (Jerusalem, Israel). ProLong Gold antifade with DAPI mounting medium was purchased from Invitrogen (Eugene, OR, USA). Nu/nu mice and folate depleted diet were purchased from Harlan (Rechovot, Israel). All tissue culture reagents were purchased from Biological Industries Ltd (Beit Haemek, Israel), unless otherwise indicated.

Methods

Synthesis of polymeric conjugates of doxorubicin

Pullulan derivatized with PEG and cysteamine (NH_2-PEG)-Pull-(Cyst), pullulan derivatized with PEG, cysteamine and FA, (FA-PEG)-Pull-(Cyst), pullulan derivatized with PEG, cysteamine and Dox, (FA-PEG)-Pull-(Cyst), and pullulan derivatized with PEG, cysteamine (Cyst), FA and Dox, (FA-PEG)-Pull-(Cyst-Dox), were synthesized according to previously published procedures [33] described in Supporting Information.

Liposomal formulation

The PEGylated liposomal doxorubicin formulation used in these studies was Doxil®, a product of Johnson & Johnson, marketed in Israel by Janssen Pharmaceuticals (Shefayim, Israel) in 10 mL vials at a doxorubicin concentration of 2 mg/mL. Control drug-free PEGylated liposomes (PL) were prepared as reported by Shmeeda *et al.* [54]. Both Doxil® and control liposomes were in the mean size range of 80-100 nm. Folate-derivatized PEG_{3350}-DSPE (FA-PEG_{3350}-DSPE) was prepared as described previously [55]. Ligand post-insertion was performed as previously reported [53].Detailed procedure is reported in Supporting Information.

Dynamic light scattering and zeta potential (ζ potential) measurements

The dynamic light scattering (DLS) and ζ potential measurements were performed with a ZetaSizer Nano ZS (Malvern instruments, UK). The pullulan conjugates and the liposomes samples were diluted in 10 mM phosphate buffer at pH 7.0. The measurements of hydrodynamic diameter and ζ potential were determined at 25°C, three times for each sample.

Cell lines

Human cervical carcinoma KB cells (HeLa contaminant, LoFR-KB cell line) were purchased from ATCC (Manassas, VA, USA) and cultured in RPMI-1640 (Gibco-InVitrogen, Carlsbad, CA, USA) supplemented with 10% (v/v) heat-inactivated foetal bovine serum, 2 mM glutamine, 100 IU/mL penicillin and 100 μg/mL streptomycin. A subline of KB cells overexpressing folate receptor (HiFR-KB cell line) was cultured in FA-depleted medium (FF-RPMI) supplemented with 10% (v/v) heat-inactivated foetal bovine serum, 2 mM glutamine, 100 IU/mL penicillin and 100 μg/mL streptomycin [55]. Human umbilical vein endothelial cells (HUVEC) were purchased from Lonza (Visp, Switzerland) and cultured in EGM-2 medium (Lonza, Visp, Switzerland). All Cells were grown at 37 °C; 5% CO_2.

Folate Competition Study

HiFR-KB, LoFR-KB or HUVEC cells were seeded at a concentration of $1x10^6$ cells/well in a 24 well plate, in 0.5 mL of RPMI (for LoFR-KB), FF-RPMI (for HiFR-KB cells) or EMB-2 (for HUVEC), with cold FA, (FA-PEG)-Pull-(Cyst) or folated drug-free PEGylated liposomes (PL-FA) at 2 μM FA-equivalent dose. Following 3 h of incubation, 10 μL of [^{3}H]FA (5 μCi/mL, 10 μM, diluted to a final concentration in each well 0.2 μM) were added to each well. Following additional 3 h of incubation, the medium was removed, the cells harvested with trypsin and the suspension was centrifuged. The supernatant was discarded and the pellet washed 3 times with 10 mM phosphate buffer, 0.15 M NaCl (PBS), pH 7.4. After the last wash, each sample was treated overnight with 500 μL of 0.5 N NaOH, followed by neutralization with 0.5 N HCl. After 30 min, 600 μL of the suspension was added to 3 mL of scintillation fluid and the amount of radioactivity was determined (Tri-Carb® 2100TR liquid scintillation counter, Waltham, MA, USA).

Intracellular trafficking of pullulan conjugate and PEGylated liposomal doxorubicin

HiFR-KB cells were seeded on sterile 13 mm cover glasses in a 24 wells plate (1.5×10^5 cells/0.5 mL per well in FF-RPMI) 24 h before incubation with conjugates. HiFR-KB cells were incubated with 200 nM Dox, or Dox-equivalent of (FA-PEG)-Pull-(Cyst-Dox), (NH_2-PEG)-Pull-(Cyst-Dox), PLD or PLD-FA for different times (5 min, 30 min, 4 h, 24 h), then washed three times with cold PBS, pH 7.4, fixed with 3.5% paraformaldehyde for 15 min at room temperature (RT) and washed again with PBS. For counter staining, cells were permeabilized with 0.1% Triton X-100 for 3 min and rinsed with PBS, pH 7.4. For confocal imaging of conjugate cellular uptake by KB cells, cover glasses were mounted by ProLong Gold anti-fade with DAPI mounting medium. All slides were kept at 4°C in dark until confocal microscopy analysis was performed.

Confocal microscopy

Cellular uptake, internalization and colocalization of conjugates and liposomes were monitored utilizing a Leica TCS SP5 confocal imaging systems with 60x oil objectives. All images were taken using a multi-track channel acquisition to prevent emission cross-talk between fluorescent dyes. Single XY, XZ plane-images were acquired in 1024×1024 resolution. Images from Z stack acquisition were processed as separate channels using Huygens® deconvolution software and merged as a single image.

Cell viability studies

The HiFR-KB cells were seeded in 96-well tissue culture plates at a density of 2×10^3 cells/well in FF-RPMI. After 24 h, the culture medium was replaced with 100 μL of medium containing serial increasing concentrations (0.01 nM–100 μM) of Dox or Dox-equivalent

(FA-PEG)-Pull-(Cyst-Dox), (NH_2-PEG)-Pull-(Cyst-Dox), PLD, PLD-FA. The plates were incubated for 72 h (long-term exposure) or alternatively after 1 h (short-term exposure) the treatments were removed, and the cells washed with 200 μL of PBS, pH 7.4. The cells incubated for 1 h were further incubated for 72 h in drug free medium. After 72 h, 20 μL of a 5 mg/mL MTT solution in PBS, pH 7.4, was added to each well. The plates were incubated for 5 h at 37°C, and then the medium was replaced with 200 μL of DMSO. The plates were maintained under gentle stirring for 1 h, and the optical absorbance was measured at 570 nm using SpectraMax $M5^e$ Microplate Reader (Molecular Devices, LLC. Sunnyvale, CA, USA)

Anti-angiogenic activity on HUVEC

Endothelial cell proliferation assay

HUVEC (1.5×10^4 cells/0.5 mL per well) were plated onto 24 well plates in EBM-2 supplemented with 5% FBS. After incubation for 24 h, cells were exposed to serial concentrations of Dox or Dox-equivalent (FA-PEG)-Pull-(Cyst-Dox), (NH_2-PEG)-Pull-(Cyst-Dox), PLD, PLD-FA dissolved in EGM-2. Following 72 h of incubation, HUVEC were trypsinized and counted by Z1 Coulter® Particle Counter (Beckman Coulter™). Alternatively the cells were treated for 30 min, then incubated for 72 h in EGM-2 drug-free medium and counted by Coulter Counter.

Evaluation of anti-tumor activity and toxicity of the conjugates

All animal procedures were performed in compliance with Tel Aviv University, Sackler School of Medicine guidelines and protocols approved by the institutional animal care and use committee (IACUC).

***In vivo* tumor targeting evaluation**

Nu/nu female mice (6 week old) were inoculated to the right flank with 1×10^6 HiFR-KB cells. Mice were fed with a folate-free diet 7 days prior to tumor inoculation and the standard diet was resumed 2 days after first treatment. Mice bearing ~40 mm^3 tumors were treated intravenously (i.v.) with three weekly injections of 5 mg/kg (cumulative dose 15 mg/kg) of Dox or Dox-equivalent of (FA-PEG)-Pull-(Cyst-Dox), (NH_2-PEG)-Pull-(Cyst-Dox), PLD, PLD-FA. Tumor progression was monitored by caliper measurement ($width^2$ x length x 0.52) twice a week. Body weight and tumor size were monitored twice a week (n = 8 mice/group). In a second experiment, nu/nu female mice were inoculated in the right flank with 1×10^6 HiFR-KB cells. Mice were fed with a folate-free diet 7 days prior to tumor inoculation and the standard diet was resumed 2 days after first treatment. Mice bearing ~40 mm^3 tumors were treated i.v. every other day with 5 mg/kg Dox-equivalent (cumulative dose 15 mg/kg) of Dox or (FA-PEG)-Pull-(Cyst-Dox), (NH_2-PEG)-Pull-(Cyst-Dox), PLD, PLD-FA. Tumor progression was monitored by caliper

measurement (width^2 x length x 0.52) every other day. Body weight and tumor size were monitored every other day (n = 12 mice/group, average of two independent experiments). In a third experiment, mice nu/nu female mice were inoculated in the right flank with 1 × 10^6 HiFR-KB cells. Mice were fed with a folate-free diet 7 days prior to tumor inoculation and the standard diet was resumed 2 days after first treatment. Mice bearing ~40 mm^3 tumors were treated i.v. with six injections (on day 1, 2, 3 and 6, 7, 8) each of 5 mg/kg (cumulative dose 30 mg/kg) of Dox or (FA-PEG)-Pull-(Cyst-Dox), (NH_2-PEG)-Pull-(Cyst-Dox) (Dox-equivalent dose). Tumor progression was monitored by caliper measurement (width^2 x length x 0.52) every other day. Body weight and tumor size were monitored every other day (n = 6 mice/group). In all the experiments, humanitarian end point was set at 20% body weight loss, or 800-1000 mm^3 tumor size. All the i.v. injections were performed via the tail vein. The pullulan polymers and liposomes were all dissolved in sterile saline. A control group was injected with saline.

Echocardiography Examination

Mice treated every other day with 5 mg/Kg (cumulative dose 15 mg/Kg) of Dox or Dox-equivalent dose of (FA-PEG)-Pull-(Cyst-Dox), (NH_2-PEG)-Pull-(Cyst-Dox), PLD, PLD-FA, were anesthetized with 2% isoflurane and echocardiograms were performed with a commercially available mouse 2D-echocardiography system (Vevo 2100, VisualSonics, Toronto, Canada) equipped with 35 MHz phased array transducer. Transthoracic echocardiography was performed, 10 days after the last treatment, as previously described [56]. An experienced technician, blinded to the treatment groups, performed all measurements that were averaged for 3 consecutive cardiac cycles.

Histological analysis

After functional evaluation, animals were euthanized with an overdose of pentobarbital and hearts were perfused with 4% formaldehyde (15 mmHg) for 10 min. Hearts were harvested, sectioned and adjacent blocks were embedded in paraffin, sectioned into 5-µm slices. To evaluate pathological changes in cardiac morphology and structure, heart sections were stained with Masson’s Trichrome.

Statistical methods

Data were expressed as mean ± SD for *in vitro* assays or ± SEM for *in vivo*. Statistical significance was determined using two-way ANOVA. Because of the relatively small number of animals in each echocardiography study, echocardiography and histology data were compared by one-way ANOVA with Tukey's test. The Kaplan-Meier method and Log-rank tests were used to evaluate survival.

RESULTS

Synthesis and characterization of drug delivery systems of doxorubicin

The Dox- and FA-derivatized pullulan [(FA-PEG)-Pull-(Cyst-Dox); Figure 1A] and Dox-derivatized pullulan [(NH_2-PEG)-Pull-(Cyst-Dox)] were synthesized according to the procedure reported before [33]. Spectrophotometric analyses showed that the (NH_2-PEG)-Pull-(Cyst) contained 4.8 mol% FA and 3.4 mol% Dox, with respect to the glucose units, while (NH_2-PEG)-Pull-(Cyst) contained 2.1 mol% Dox. Control drug-free pullulan derivatives with FA [(FA-PEG)-Pull-(Cyst); 5 mol% FA)] or without FA [(NH_2-PEG)-Pull-(Cyst)] were also synthesized. Table I reports the complete composition of the polymer conjugates. The main physico-chemical properties, namely apparent size and ζ potential are reported in Table III. Both pullulan bioconjugates displayed similar molecular weight (~ 150 kDa apparent molecular weight, polydispersity - Mw/Mn 1.8) and negative ζ potential.

The folated liposomal formulation of Dox (PLD-FA, Figure 1B) was prepared via ligand post insertion of folate conjugated DSPE on the surface of commercial Dox-loaded PEGylated liposomes (Doxil®). The Dox and FA contents in PLD-FA were 13.9 mol% and 0.3 mol%, respectively. Dox content in the non-folated PLD was 14.5 mol%. Drug-free, FR-targeted liposomes (PL-FA), and drug-free non-folated liposomes (PL) were also prepared as references. Table II reports the composition of liposomal formulations. The physico-chemical properties of the liposomal formulations, namely size and ζ potential are reported in Table III. All liposomal formulations displayed similar size profiles (~ 80 nm) and negative ζ potential.

FR-targeted drug delivery systems are internalized via receptor-mediated uptake in FR-overexpressing cells.

The FR receptor-mediated cell uptake selectivity of folated and non-folated delivery systems was investigated by competitive studies according to a validated protocol. Following three hours of incubation with [^{3}H]FA, KB cells cultured in folate-depleted media (HiFR-KB cells) were highly radioactive (17259 ± 2192 dpm), while KB cells cultured in regular RMPI (LoFR-KB) and HUVEC grown in EBM-2 medium were negligibly radioactive (125 ± 50 dpm and 25 ± 1.6 dpm respectively) (compared with HiFR-KB, $p<10^{-6}$). The competitive incubation of HiFR-KB cells with [^{3}H]FA and cold (non-radiolabelled) FA, (FA-PEG)-Pull-(Cyst) or PL-FA showed a dramatic decrease in cell radioactivity ($p<10^{-9}$) (Figure 2A) suggesting that the nanoconjugates are internalized via FR-mediated endocytosis.

Dox internalization kinetics to HiFR-KB cells was assessed by laser scanning confocal microscopy (LSCM). Free Dox was rapidly internalized by diffusion into cells, and localized in the nucleus (Figure 2B). (FA-PEG)-Pull-(Cyst-Dox) conjugate internalized within 5 min into the cells (Figure 2B), in agreement with our previously published results

in live cells [33]. Following endosomal escape and the release of free Dox from the polymer, Dox localized in the nucleus within 240 min (Figure 3). Non-folated (NH_2-PEG)-Pull-(Cyst-Dox) conjugate undergoes slower internalization (240 min, Figure 2B). Similarly, the liposomal cell internalization was found to depend on the presence of FA. A significant amount of PLD-FA internalized in 4 h, while the non-folated PLD was not taken-up by the cells at this time.

(FA-PEG)-Pull-(Cyst-Dox) conjugate and PLD-FA inhibit the proliferation of human cervical carcinoma overexpressing the folate receptor (HiFR-KB) and human umbilical vein endothelial cells (HUVEC).

The pharmacological activity of (FA-PEG)-Pull-(Cyst-Dox) and PLD-FA was evaluated using HiFR-KB cells and HUVEC. Free Dox was used as control. Studies were carried out either by prolonged or by short-term (72 h and 1 h, respectively) cell incubation with the Dox formulations. In the case of short-term incubation, after 1 h exposure to treatment the medium was replaced with fresh medium followed by 72 h of continued culture. IC_{50} values were graphically extrapolated from the viability plots reported in Figure 3 and approximated to the closest round value.

HiFR-KB cell growth inhibition curves obtained by prolonged and short-term drug exposure are shown in Figures 3A-3B, and IC_{50} values are summarized in Table IV. Following 72 h exposure to treatments, IC_{50} values of (FA-PEG)-Pull-(Cyst-Dox) and (NH_2-PEG)-Pull-(Cyst-Dox) were about 50 and 5000 fold higher than free Dox, respectively (significant difference between folated and non-folated pullulan bioconjugates at $p<10^{-4}$). IC_{50} values obtained following short-term exposure to (FA-PEG)-Pull-(Cyst-Dox) and (NH_2-PEG)-Pull-(Cyst-Dox) were 80 and 400 fold higher compared to free Dox, respectively (significant difference between folated and non-folated pullulan bioconjugates $p<10^{-7}$). IC_{50} values obtained following short-term cell incubation of PLD-FA and PLD were similar to those obtained with the pullulan bioconjugates, while the prolonged cell incubation with PLD or PLD-FA resulted in 275-fold higher IC_{50} compared to free Dox (p=0.005).

Results of a similar experiment evaluating the inhibitory effect of the formulations on HUVEC proliferation are summarized in Table IV. IC_{50} values of long-term exposure to (FA-PEG)-Pull-(Cyst-Dox) and (NH_2-PEG)-Pull-(Cyst-Dox) were about 20 and 400 fold higher than that obtained with free Dox, respectively (significant difference between folated and non-folated pullulan bioconjugates at $p<10^{-14}$) (Figure 3C), while following short-term incubation, it was about 5 and 200 fold higher than Dox (significant difference between folated and non-folated pullulan bioconjugates at $p<10^{-5}$) (Figure 3D). The IC_{50} values obtained following prolonged cell exposure to PLD-FA and PLD were 150 and 300 fold higher than Dox (significant difference between PLD-FA and PLD at $p<10^{-5}$) (Figure 3C). Short-term cell exposure with PLD-FA and PLD resulted in about 3 and 200 fold

higher IC_{50} compared to free Dox, respectively (significant difference between PLD-FA and PLD at $p<10^{-5}$) (Figure 3D).

The therapeutic index of (FA-PEG)-Pull-(Cyst-Dox) conjugate and PLD-FA depends on their dosing schedule *in vivo*

In vivo antitumor efficacy was evaluated using nu/nu mice inoculated with human HiFR-KB cells. The animals were fed with folate-depleted diet for 7 days before tumor cell inoculation and 7 days following tumor inoculation, in order to upregulate the expression of FR on cancer cells. Mice were treated three times with the Dox formulations according to two treatment schedules: a weekly and an alternate day i.v. administration. In addition, the pullulan conjugates, which were found non-toxic under the dosage regimen of previous experiments were injected six times at a daily dosing schedule (injections on days 1, 2, 3, 6, 7, 8). Free Dox was also administered as a reference.
Three weekly i.v. injections of 5 mg/Kg Dox-equivalent dose of PLD and PLD-FA strongly inhibited tumor growth rate and prolonged survival compared to saline (time by treatment interaction resulted at p=0.046 and Log-rank p=0.004 for PLD, p=0.011 for Dox and p=0.0002 for PLD-FA compared with saline).The folated liposomal formulation displayed higher activity and survival rate compared to the non-folated counterpart. The pullulan conjugates, at this dosing schedule, did not show any anticancer activity or advantage compared to saline (Figure 4A, C). With this treatment regimen, all the formulations were safe and did not cause body weight loss (Figure 4B).

Three treatments every other day with 5 mg/kg Dox-equivalent dose of Dox, (FA-PEG)-Pull-(Cyst-Dox), (NH_2-PEG)-Pull-(Cyst-Dox), PLD or PLD-FA inhibited tumor growth rate (Figure 5A). The ability of PLD and PLD-FA to decrease tumor size appeared only 6 days after treatment initiation, probably as a result of increased half-life and sustained drug release from these liposomal formulations. Tumor growth inhibition was seen as soon as 3 days following treatment initiation with the pullulan conjugates. (FA-PEG)-Pull-(Cyst-Dox) showed a slight advantage compared to the non-folated (NH_2-PEG)-Pull-(Cyst-Dox) up to 10 days after treatment discontinuation (Figure 5B). This dosing schedule caused several toxic deaths for the animals treated with Dox and PLD, while PLD-FA had a lower toxicity, in accordance with previous reports [53] (Figure 5D). For these groups, body weight loss (≥10% of initial weight) was reported for the mice treated with Dox, PLD and PLD-FA (Figure 5C). However, this toxicity was reversible following treatment discontinuation resulting in longer overall survival compared with saline for the groups that were initially treated with Dox (p=0.05), PLD (p=0.0005) and PLD-FA (p=0.0046) and survived the days of treatment (Figure 5E). (FA-PEG)-Pull-(Cyst-Dox) and (NH_2-PEG)-Pull-(Cyst-Dox) inhibited tumor growth to a lesser extent but did not cause body weight loss (Figure 5C). These findings suggested that the dose of (FA-PEG)-Pull-(Cyst-Dox) and (NH_2-PEG)-Pull-(Cyst-Dox) can further be increased in order to obtain a better therapeutic response with an improved therapeutic index.

As the pullulan conjugates were safe at the previous studies, a third experiment was undertaken at a schedule administration of six i.v. injections of 5 mg/kg Dox-equivalent dose of Dox, (FA-PEG)-Pull-(Cyst-Dox) and (NH_2-PEG)-Pull-(Cyst-Dox). This dosing regimen improved the anticancer activity of the pullulan conjugates. In particular, the FR-targeted (FA-PEG)-Pull-(Cyst-Dox) showed tumor growth inhibition of 96% compared to the saline control ($p<10^{-12}$), and 94% compared to the non-folated polymer Pull-PEG-Dox on day 19 (Figure 6A) when all treatment groups were still in the study. All treatments, Dox, (FA-PEG)-Pull-(Cyst-Dox) and (NH_2-PEG)-Pull-(Cyst-Dox), caused body weight loss to a different extent (up to 20%, 13% and 9%, respectively) (Figure 6B). The body weight loss was non-reversible for mice treated with free Dox and all the mice treated with Dox died soon after the last treatment (Figure 6C). On the contrary, the mice treated with the pullulan conjugates gained weight immediately after the last treatment, and the survival was significantly extended compared to Dox-treated mice and the saline group (p=0.0018 and p=0.0014 respectively) (Figure 6C). The higher cumulative dose and the more frequent injections significantly improved the outcome of this dosing regimen for (FA-PEG)-Pull-(Cyst-Dox), suggesting not only a reduction of toxicity, but also a clear beneficial effect of FR-targeting compared to the non-folated (NH_2-PEG)-Pull-(Cyst-Dox) conjugate.

Pullulan conjugates and liposomal formulations attenuate Dox-induced cardiotoxicity

Preliminary results from echocardiography study showed that the animals treated with Dox (three times every other day, cumulative dose of 15 mg/kg), developed left ventricle (LV) dysfunction, with an increase in LV systolic area compared to the animals treated with saline (Figure 7A). Furthermore, animals treated with free Dox experienced the lowest ejection fraction (Figure 7B). Examination of the slides stained with Masson-Trichrome showed that LV from Dox-treated animals were enlarged (Figure 7C) (n=4). Mice treated with saline, liposomal formulations or pullulan conjugates developed less adverse LV remodeling, with smaller LV area and greater wall thickness, compared with those treated with Dox. Histological staining of hearts with Masson-Trichrome revealed that left ventricle average surface area was 3.83 ± 1.00 mm^2 for saline, 3.76 ± 1.2 mm^2 for PLD and 2.72 ±1.2 mm^2 for PLD-FA, 4.00 ± 1 mm^2 for (NH_2-PEG)-Pull-(Cyst-Dox) and 3.72 ± 0.72 mm^2 for (FA-PEG)-Pull-(Cyst-Dox), 5.55 ± 0.44 mm^2 for Dox (p=0.08).

DISCUSSION

Two different Dox delivery systems, liposomal formulations (PLD and PLD-FA) [22, 57] and pullulan conjugates [(NH_2-PEG)-Pull-(Cyst-Dox) and (FA-PEG)-Pull-(Cyst-Dox)] [33], have been compared *in vitro* and *in vivo* in order to assess the advantages and disadvantages of their use for tumor targeting. As in other comparative studies [58, 59], we evaluated the two DDS on the basis of Dox-equivalent concentrations.

The pullulan conjugates were designed to obtain supramolecular systems with suitable physico-chemical and biopharmaceutical properties for non-selective blood circulation and extravasation-dependent delivery as well as receptor-targeted Dox delivery to solid tumors. Due to their smaller size and “elastic spaghetti coil-like” structure compared to the globular particulated liposomes, polymers can easily penetrate into cancer tissue though the leaky vasculature [22]. Nevertheless, for the same structural reasons, polymer bioconjugates undergo faster clearance compared to PEGylated liposomes. FA was conjugated to the polymer backbone [(FA-PEG)-Pull-(Cyst-Dox)] to endow a derivative with receptor-mediated tumor targeting ability. Dox was conjugated through a pH-sensitive bond that can be selectively cleaved under acidic conditions in the lysosomes, bestowing biopharmaceutical stability in non-target tissues, namely in the bloodstream, and site selective intracellular drug release.

Doxil® is a PEGylated liposomal formulation of Dox, approved for the treatment of breast cancer, ovarian cancer, multiple myeloma, and Kaposi’s sarcoma. This vesicular carrier allows for high Dox loading, while PEG on the liposome's surface conveys stealth properties prolonging its plasma half-life, which is related to the accumulation in the tumor tissue [22]. Similarly to (FA-PEG)-Pull-(Cyst-Dox), the commercial formulation decoration with FA moieties was performed to bestow liposomes with receptor-mediated targeting properties.

The polymeric and liposomal formulations differ in the amount of FA loading. Each chain of (FA-PEG)-Pull-(Cyst-Dox) bears an average of 4.8 FA units, while each PLD-FA is decorated with about 100-250 FA molecules per vesicle [55]. Considering the molar composition of the two formulations, the Dox:FA ratio in the pullulan formulation is ~0.7, while it is ~50 in the liposomes, due to the high Dox loading. Nevertheless, previous studies showed that these compositions yielded delivery systems with suitable biopharmaceutical features and few preliminary data showed their potential therapeutic efficiency. The different payloads of FA guarantees the binding to the FR for both the formulations, as shown in the in vitro binding assays. This is in agreement with other formulations bearing folic acid that show that this loading degree guarantees binding to FR. It is worth to note that studies reported in the literature showed that the optimal binding can be achieved at even lower folic acid loading [60, 61]. However, the optimal degree of surface substitution reasonably depends on the overall composition and physical properties of the DDS, including length of PEG used as spacer.

First, we investigated the targeting properties conveyed by FA to the pullulan and liposomal formulations. FA is a small molecule widely used to achieve tumor targeting by direct conjugation to several anticancer agents [62-64] or to colloidal high molecular weight DDS such as polymer therapeutics [65, 66] and liposomal formulations [54, 67] as it can promote tumor cell receptor-mediated internalization of drugs and colloidal drug carriers [33, 55]. Accordingly, FA functionalized colloidal DDS have been found to exhibit FR-mediated cytotoxicity and *in vivo* antitumor effect [68, 69]. Interestingly, the conjugation of FA to a low MW agent via a short linker compared to that via a series of

long linkers (PEG_{5000}, PEG_{20000} and PEG_{60000}) gave the best results in terms of improving tumor penetration rate and accumulation [70].

The ability of FA to promote receptor-mediated internalization of drugs and colloidal drug carriers was shown in previous studies [33, 55] and was confirmed by a competition assay on human cervical carcinoma KB cells, which overexpress the folate receptor when cultured in folate-depleted medium.

HiFR-KB cells highly internalize the radioactive FA, ([^{3}H]FA), while the internalization is negligible in LoFR-KB cells. Competitive studies performed by simultaneous cell incubation with [^{3}H]FA and (FA-PEG)-Pull-(Cys) or PL-FA showed that the intracellular radioactivity dramatically decreases (Figure 2A) demonstrating that the folated DDS compete with the radioactive FA for receptor-binding and cell internalization.

The internalization profiles of the DDS in HiFR-KB were followed by confocal microscopy, recording the fluorescence of Dox conjugated to the polymers or encapsulated in the liposomes. As previously reported [33], Dox undergoes rapid cellular internalization (5 min), showing colocalization with DAPI in the nucleus within 30 min (Figure 2B). After 4 h incubation with 200 nM Dox, high levels of cell death occurred. The non-folated DDS, (NH_2-PEG)-Pull-(Cyst-Dox) and PLD, were not yet internalized within 4 h, indicating that these systems undergo slow endocytosis. The internalization of the FR-targeted pullulan conjugate, (FA-PEG)-Pull-(Cyst-Dox), was observed within 5 min of incubation [33], correlating to the fast FR-mediated endocytotic mechanism. Following endosomal escape, the free drug is released to the cytoplasm and then gains access to the nucleus within 4 h. The uptake of PLD-FA required longer incubation with the HiFR-KB cells compared to the (FA-PEG)-Pull-(Cyst-Dox) presumably because of structural constraints and slower internalization process.

The dynamic light scattering (DLS) analysis showed two populations of pullulan bioconjugates in buffer, where one population is small and the size of the other population is larger than the liposomes. Previous studies showed that the bioconjugate assembling is mainly due to the presence of folic acid along the backbone that promotes hydrophobic interactions. Therefore, it is possible that polymer bioconjugates undergo disassembling and unfolding in the physiological medium of cell incubation and this new extended conformation may favor the FA exposure for FR recognition and cell internalization. Liposomes, though smaller than the bigger population of the pullulan bioconjugates in buffer, maintain their vesicular structure and that may slow down their FR-mediated transit through the cell membrane.

The *in vitro* cell selectivity and anticancer activity of the DDS was shown with human cervical carcinoma HiFR-KB cells, which overexpress the folate receptor. By long-term exposure (72 h cell incubation), the FR-targeted pullulan derivative was much more active than the non-folated counterpart. After long-term exposure, the FR-targeted pullulan conjugate, (FA-PEG)-Pull-(Cyst-Dox), exhibited an IC_{50} of 20 nM (Figure 3A, Table III). The IC_{50} value of (NH_2-PEG)-Pull-(Cyst-Dox) (2000 nM) was 100-fold higher than that of (FA-PEG)-Pull-(Cyst-Dox) while the IC_{50} of free Dox was 0.4 nM.

In LoFR-KB cells, after 72 h incubation, the IC50 value of (NH2-PEG)-Pull-(Cyst-Dox) (2000 nM) was 50-fold higher than that of (FA-PEG)-Pull-(Cyst-Dox) (Figure S1). The different cytotoxicity profiles resulting from long-term treatment with FR-targeted and non-folated pullulan conjugates might be ascribed to a combination of events, which include the different internalization rate and pathway, as well as the different drug release kinetics. These events reflect the conjugate composition, namely the presence or absence of the targeting agent and the drug loading. Indeed, the folated conjugate can be rapidly taken-up by the cells through a receptor-mediated process that involves the caveolar pathway, while its non-folated counterpart is taken-up by cells via a non-selective endocytotic mechanism. Furthermore, although the long-term incubation may minimize the differences in cell internalization related to the different uptake processes, it should be noted that the pullulan conjugates have negative ζ potential, -5.43 ± 0.84 mV for (FA-PEG)-Pull-(Cyst-Dox) and -4.94 ± 0.64 mV for the non-folated polymer (NH_2-PEG)-Pull-(Cyst-Dox). Therefore, the non-folated conjugate interaction with the negative surface of the cells is limited due to charge repulsion and thus, non-selective endocytosis of this derivative can be further inhibited.

Finally, according to the bioconjugate design, the pullulan bioconjugates were found to be stable under physiological medium [33], indicating that Dox is not released in the extracellular medium where the non-folated derivative stay longer than the rapidly cell internalized folated bioconjugate, thus preventing cell uptake of free Dox. In contrast to the pullulan bioconjugates, long-term incubation of HiFR-KB cells with PLD and PLD-FA yielded similar IC_{50} values for both (200 nM). Although PLD-FA is more rapidly and extensively internalized via the FR than PLD, the long-term cell exposure to the formulation can yield similar cytotoxic activity possibly due to slow drug release in the extracellular medium via leakage from the liposomal formulation and subsequent cellular internalization of free drug.

Similar results were obtained on the LoFR-KB cells treated with the liposomal formulations (Figure S1). The short-term exposure (1 h incubation of HiFR-KB cell with the Dox formulations followed by 72 h cell incubation in drug-free medium) (Figure 3B) also shows the effect of FA on cell targeting and uptake. Following short-term exposure, both FR-targeted conjugate and FR-targeted liposome exhibited higher activity (5-fold) compared to the non-folated carriers (Table IV)**.** Long-term exposure discriminates better between FR-targeted and non-folated pullulan conjugates than between the liposomal formulations (Figure 3A).These results confirm the data obtained by long-term cell incubation with the pullulan conjugates and show that the bioconjugate selectivity is well-observed by prolonged cell exposure. The differences displayed between FR-targeted and non-folated liposomes confirm the selective and faster cell uptake of the former observed by competitive assay and confocal microscopy, and indicate that in 1 h the drug is not significantly released in the extracellular medium.

Next, the anti-angiogenic potential of the pullulan conjugates and the liposomal formulations was evaluated *in vitro* on HUVEC. Unexpectedly, the cytotoxicity results

obtained by long-term and short-term cell treatment were intriguing as they resembled the results obtained with HiFR-KB cells, suggesting that FA promotes the HUVEC uptake of the FR-targeted DDS. Actually, even though two studies reported that HUVEC express the FR [71, 72], our findings from the internalization assay with [^{3}H]FA showed that HUVEC do not have strong capacity to internalize the folated carriers (Figure 2A). We hypothesized that FA could be toxic to HUVEC, but treatment with FA alone did not inhibit HUVEC proliferation (Figure S2). Therefore, the data obtained in this study seems to suggest that in the case of HUVEC, FA activates a cell uptake process, which parallels the one involved in the FR-mediated uptake of [^{3}H]FA. Indeed, It has been reported before that FA has anti-angiogenic activity on endothelial cells, inhibiting proliferation and reducing tube formation, although at high concentrations [73]."

Since we found increased HUVEC cytotoxicity for the folated-polymeric systems, we evaluated the anti-angiogenic potential of all formulations with an *in vitro* capillary-like tube formation assay (Figure S4). Dox is not reported to inhibit the tube formation and neither the liposomal formulations nor the polymeric conjugates were able to enhance the anti-angiogenic activity. In this case, no difference was observed between the FR-targeted and non-folated systems as none of the compounds evaluated were active.

Then, the *in vivo* antitumor efficacy of all four drug delivery systems was examined in the human KB nu/nu mouse model. Tumor growth, weight loss and survival rate were assessed. In the first study, following three once-weekly treatments, both PLD and PLD-FA exhibited high antitumor efficacy reducing the tumor growth rate and increasing survival, as compared to the control (untreated) animals, where the folated liposomal formulation was even more efficacious than the non-folated formulation. This improved activity of the folate receptor-targeted liposomal formulation has been reported earlier for a different dosing regimen of Dox (single injection of 10 mg/kg versus our three weekly 5 mg/kg regimen at a different folic acid loading of 0.03% versus our 0.3%) [61] and route of administration (i.p. *versus* our i.v.) [74]. Following our dosing regimen, the non-folated liposomes showed similar tumor growth rate inhibition, body weight decrease and survival rate as free Dox. Our results seem to contradict previous reports, in which non-targeted liposomes showed improved anticancer activity compared with free Dox [53, 61], however the dissimilar results might be ascribed to the different treatment conditions, namely the administration regimen. In this case, the two pullulan bioconjugates were ineffective showing similar tumor growth and animal survival rate profiles as the mice treated with saline. No weight loss was registered during the three weeks of the treatment for all the groups. The higher efficacy of the liposomal formulations as compared to the polymer bioconjugates can be explained by the different pharmacokinetic profiles of the two formulations. Previous studies showed that the bioconjugates undergo relatively rapid clearance from the bloodstream as about 50% of the injected formulation disappears from the circulation in about 2 h [33], while the half-life of PEGylated liposomes in mice is 19 h [75]. The prolonged stability in the bloodstream of the liposomes are reflected in higher accumulation in the tumor mass than found with the polymer bioconjugates.

The previous experiment was designed according to the classical dosing schedule and optimized for the long-circulating liposomal formulations. A second study (Figure 5), with a dosing schedule more adapted to polymer therapeutics which have a shorter half-life pharmacokinetic profile [33] was performed, administering a total of 3 treatments every other day, *i.e.* the same cumulative dose but using a higher dose intensity. Although free Dox, PLD and PLD-FA were effective in reducing tumor size (Figure 5A), severe weight loss and a high number of toxic deaths were observed in animals treated with these compounds (Figure 5B, C). Surprisingly, under this dosage regimen, the folated liposomes were less effective than the non-folated formulation. This seems to indicate that frequent administration of the Dox-loaded liposomes may cause a continuous feeding of the tumor, where the targeting properties become irrelevant, while the presence of the targeting agent can even reduce the accumulation of the carrier in a massive tumor mass. The toxicity of the liposomal formulation was reversible once the treatment was discontinued, and the overall survival was prolonged both for PLD and PLD-FA for those mice that survived the treatment period, even though PLD-FA reduced the number of toxic deaths compared to the non-folated PLD (Figure 5C). Both pullulan conjugates, [(FA-PEG)-Pull-(Cyst-Dox) and (NH_2-PEG)-Pull-(Cyst-Dox)] were not toxic (Figure 5B, C), and displayed similar antitumor efficacy to free Dox without relevant differences between the folated and non-folated form (Figure 5A). These data taken together, suggest that a higher dose of pullulan conjugates, as opposed to the liposomal formulations, can be administered in order to obtain higher anticancer activity and limited toxicity.

Accordingly, in the third study, mice were treated with the polymer conjugates with an even more intense dosing schedule (three daily injections and another three daily injections after 3 more days) and with a higher cumulative dose (30 mg/kg Dox-equivalent dose). Here, the FR-targeted (FA-PEG)-Pull-(Cyst-Dox) becomes an effective anticancer agent, reducing tumor growth up to 94% compared to non-treated mice (Figure 6A). At this dosing schedule, the mice treated with the free Dox showed high irreversible weight loss (up to 20%) (Figure 6B), leading to rapid toxic death of all the mice treated with Dox (Figure 6C). On the contrary, the mice treated with the pullulan-based delivery systems showed moderate and reversible body weight loss following treatment discontinuation (Figure 6B). The polymeric carriers improved survival up to 50 days following treatment initiation (Figure 6C).

Cardiotoxicity is one of the most severe adverse effects caused by Dox treatment, and several parameters have been reported to correlate with myocarditis induced by treatment with the free drug [76, 77]. The ability of drug delivery systems to reduce cardiotoxicity was evaluated by echocardiography and histological examination of the hearts of the treated animals by an experienced radiology technician and cardiologist. The echocardiography scan was performed on a small number of mice (n=2-3/group), due to high animal mortality and therefore, the statistical evaluation of the experiment is limited. Nevertheless, the echocardiography scan and the histological analysis of the hearts (including those who died during the experiment) suggest that all liposomal and

polymeric formulations tested in this study reduce the cardiotoxicity related to Dox therapy. For PLD, this is well known from clinical experience [24, 78]. The mice treated with free Dox developed adverse remodeling, especially in the systolic phase (Figure 7A), and impaired contractility reflected by impaired left ventricle ejection fraction (EF) (Figure 7B), compared with mice treated with saline and with the drug delivery systems. In particular, the hearts of the mice treated with PLD, PLD-FA, (NH_2-PEG)-Pull-(Cyst-Dox) and (FA-PEG)-Pull-(Cyst-Dox) (Figure 7C) showed smaller left ventricle (LV) volume and greater ventricle wall thickness, compared to free Dox-treated mice, suggesting that liposomal and polymeric nanomedicines are safer than free Dox and can prevent Dox-induced cardiotoxicity as already shown clinically for PLD [78]. These encouraging results suggest that the two types of delivery systems evaluated here can enhance anticancer activity, reduce or even abrogate toxicity, leading to prolonged survival if administered using an appropriate dosing schedule.

CONCLUSION

Much effort has been invested in the quest for the best ligand for selective targeting of DDS to a tumor tissue. However, a more pressing question arising – is whether it is effective at all to use a specific targeting moiety and if so, can we generalize this approach to various DDS? This study constitutes the first side-by-side comparison of two receptor-targeted ligand-bearing systems, evaluating a polymeric *versus* a liposomal system in the same models. Via a simple and effective chemical protocol, it is possible to conjugate folic acid to different nanocarriers, maintaining the binding affinity of the ligand to the folate receptor, and exploiting its targeting properties to promote the internalization of the carriers. The four formulations designed display potent *in vivo* pharmacological activity while reducing the toxic effects of the free drug.

FR-targeted polymer therapeutics and liposomal formulations can serve as precision nanomedicines for the treatment of a variety of cancers and other difficult-to-treat diseases where overexpression of the folate receptor occurs, such as polycystic kidney disease, and inflammatory diseases. For polymeric constructs, the dosing regimen and the dosing intensity strongly affect the therapeutic index and reveals a major therapeutic advantage for the FR-targeted formulation.

ACKNOWLEDGMENTS

A.S. thanks Tel Aviv University Center for Nanoscience and Nanotechnology for an excellence postdoctoral fellowship. This study was partially supported by The European Research Council (ERC) Consolidator Award (617445—PolyDorm), The Israel Science Foundation (Grant No. 918/14), the Swiss Bridge Award, and by grants from the Israeli National Nanotechnology Initiative (INNI), Focal Technology Area (FTA) program: Nanomedicine for Personalized Theranostics, and by The Leona M. and Harry B.

Helmsley Nanotechnology Research Fund, The Ministry of Science, Technology and Space of Israel, and the Ministry of Foreign Affair of Italy scientific cooperation grant, and The Israel Cancer Research Fund (ICRF) (RSF).

REFERENCES

[1] K. Strebhardt, A. Ullrich, Paul Ehrlich's magic bullet concept: 100 years of progress, Nat Rev Cancer, 8 (2008) 473-480.

[2] R. Duncan, R. Gaspar, Nanomedicine(s) under the Microscope, Mol Pharm, 8 (2011) 2101-2141.

[3] A. Eldar-Boock, D. Polyak, A. Scomparin, R. Satchi-Fainaro, Nano-sized polymers and liposomes designed to deliver combination therapy for cancer, Current opinion in biotechnology, 24 (2013) 682-689.

[4] H. Maeda, Tumor-selective delivery of macromolecular drugs via the EPR effect: background and future prospects, Bioconjug Chem, 21 (2010) 797-802.

[5] Y. Matsumura, H. Maeda, A new concept for macromolecular therapeutics in cancer chemotherapy: mechanism of tumoritropic accumulation of proteins and the antitumor agent smancs, Cancer Res, 46 (1986) 6387-6392.

[6] U. Prabhakar, H. Maeda, R.K. Jain, E.M. Sevick-Muraca, W. Zamboni, O.C. Farokhzad, S.T. Barry, A. Gabizon, P. Grodzinski, D.C. Blakey, Challenges and key considerations of the enhanced permeability and retention effect for nanomedicine drug delivery in oncology, Cancer Res, 73 (2013) 2412-2417.

[7] G. Gregoriadis, B.E. Ryman, Liposomes as carriers of enzymes or drugs: a new approach to the treatment of storage diseases, Biochem J, 124 (1971) 58P.

[8] E. Koren, A. Apte, A. Jani, V.P. Torchilin, Multifunctional PEGylated 2C5-immunoliposomes containing pH-sensitive bonds and TAT peptide for enhanced tumor cell internalization and cytotoxicity, J Control Release, (2011).

[9] J.M. Rosenholm, V. Mamaeva, C. Sahlgren, M. Linden, Nanoparticles in targeted cancer therapy: mesoporous silica nanoparticles entering preclinical development stage, Nanomedicine (Lond), 7 (2012) 111-120.

[10] Z.Z. Li, L.X. Wen, L. Shao, J.F. Chen, Fabrication of porous hollow silica nanoparticles and their applications in drug release control, J Control Release, 98 (2004) 245-254.

[11] E. Segal, H. Pan, P. Ofek, T. Udagawa, P. Kopeckova, J. Kopecek, R. Satchi-Fainaro, Targeting angiogenesis-dependent calcified neoplasms using combined polymer therapeutics, PloS one, 4 (2009) e5233.

[12] A. Eldar-Boock, K. Miller, J. Sanchis, R. Lupu, M.J. Vicent, R. Satchi-Fainaro, Integrin-assisted drug delivery of nano-scaled polymer therapeutics bearing paclitaxel, Biomaterials, 32 (2011) 3862-3874.

[13] G.S. Kwon, K. Kataoka, Block-Copolymer Micelles as Long-Circulating Drug Vehicles, Adv Drug Deliver Rev, 16 (1995) 295-309.

[14] B.X. Zhao, Y. Zhao, Y. Huang, L.M. Luo, P. Song, X. Wang, S. Chen, K.F. Yu, X. Zhang, Q. Zhang, The efficiency of tumor-specific pH-responsive peptide-modified polymeric micelles containing paclitaxel, Biomaterials, 33 (2012) 2508-2520.

[15] J.P. Xu, J. Ji, W.D. Chen, J.C. Shen, Novel biomimetic polymersomes as polymer therapeutics for drug delivery, J Control Release, 107 (2005) 502-512.

[16] J.S. Lee, J. Feijen, Polymersomes for drug delivery: design, formation and characterization, J Control Release, 161 (2012) 473-483.

[17] R. Duncan, The dawning era of polymer therapeutics, Nat Rev Drug Discov, 2 (2003) 347-360.

[18] D.D. Lasic, D. Papahadjopoulos, Medical applications of liposomes, Elsevier, Amsterdam ; New York, 1998.

[19] T.M. Allen, G.A. Austin, A. Chonn, L. Lin, K.C. Lee, Uptake of liposomes by cultured mouse bone marrow macrophages: influence of liposome composition and size, Biochim Biophys Acta, 1061 (1991) 56-64.

[20] D. Papahadjopoulos, A. Gabizon, Liposomes designed to avoid the reticuloendothelial system, Prog Clin Biol Res, 343 (1990) 85-93.

[21] D. Papahadjopoulos, T.M. Allen, A. Gabizon, E. Mayhew, K. Matthay, S.K. Huang, K.D. Lee, M.C. Woodle, D.D. Lasic, C. Redemann, et al., Sterically stabilized liposomes: improvements in pharmacokinetics and antitumor therapeutic efficacy, Proc Natl Acad Sci U S A, 88 (1991) 11460-11464.
[22] A. Gabizon, H. Shmeeda, H. Baabur-Cohen, R. Satchi-Fainaro, Targeting the folate receptor with liposomes and polymer therapeutics. , in: J.A. Leamon C, vol. Springer-Verlag. Heidelberg, Germany; (Ed.) Targeted Drug Strategies for Cancer and Inflammation., Springer-Verlag. Heidelberg, Germany;, 2012, pp. 217-248.
[23] S.T. Duggan, G.M. Keating, Pegylated Liposomal Doxorubicin: A Review of its use in Metastatic Breast Cancer, Ovarian Cancer, Multiple Myeloma and AIDS-Related Kaposi's Sarcoma, Drugs, 71 (2011) 2531-2558.
[24] A. Gabizon, H. Shmeeda, T. Grenader, Pharmacological basis of pegylated liposomal doxorubicin: impact on cancer therapy, European journal of pharmaceutical sciences : official journal of the European Federation for Pharmaceutical Sciences, 45 (2012) 388-398.
[25] L.W. Seymour, D.R. Ferry, D.J. Kerr, D. Rea, M. Whitlock, R. Poyner, C. Boivin, S. Hesslewood, C. Twelves, R. Blackie, A. Schatzlein, D. Jodrell, D. Bissett, H. Calvert, M. Lind, A. Robbins, S. Burtles, R. Duncan, J. Cassidy, Phase II studies of polymer-doxorubicin (PK1, FCE28068) in the treatment of breast, lung and colorectal cancer, Int J Oncol, 34 (2009) 1629-1636.
[26] L. Fiume, M. Baglioni, L. Bolondi, C. Farina, G. Di Stefano, Doxorubicin coupled to lactosaminated human albumin: a hepatocellular carcinoma targeted drug, Drug Discov Today, 13 (2008) 1002-1009.
[27] F.M. Veronese, O. Schiavon, G. Pasut, R. Mendichi, L. Andersson, A. Tsirk, J. Ford, G. Wu, S. Kneller, J. Davies, R. Duncan, PEG-doxorubicin conjugates: influence of polymer structure on drug release, in vitro cytotoxicity, biodistribution, and antitumor activity, Bioconjug Chem, 16 (2005) 775-784.
[28] P.A. Vasey, S.B. Kaye, R. Morrison, C. Twelves, P. Wilson, R. Duncan, A.H. Thomson, L.S. Murray, T.E. Hilditch, T. Murray, S. Burtles, D. Fraier, E. Frigerio, J. Cassidy, Phase I clinical and pharmacokinetic study of PK1 [N-(2-hydroxypropyl)methacrylamide copolymer doxorubicin]: first member of a new class of chemotherapeutic agents-drug-polymer conjugates. Cancer Research Campaign Phase I/II Committee, Clinical cancer research : an official journal of the American Association for Cancer Research, 5 (1999) 83-94.
[29] T. Nakanishi, S. Fukushima, K. Okamoto, M. Suzuki, Y. Matsumura, M. Yokoyama, T. Okano, Y. Sakurai, K. Kataoka, Development of the polymer micelle carrier system for doxorubicin, J Control Release, 74 (2001) 295-302.
[30] S. Danhauser-Riedl, E. Hausmann, H.D. Schick, R. Bender, H. Dietzfelbinger, J. Rastetter, A.R. Hanauske, Phase I clinical and pharmacokinetic trial of dextran conjugated doxorubicin (AD-70, DOX-OXD), Investigational new drugs, 11 (1993) 187-195.
[31] R. Duncan, Polymer conjugates as anticancer nanomedicines, Nat Rev Cancer, 6 (2006) 688-701.
[32] H. Ringsdorf, Structure and properties of pharmacologically active polymers., J. Polym. Sci, 51 (1975) 135-153.
[33] A. Scomparin, S. Salmaso, S. Bersani, R. Satchi-Fainaro, P. Caliceti, Novel folated and non-folated pullulan bioconjugates for anticancer drug delivery, European journal of pharmaceutical sciences : official journal of the European Federation for Pharmaceutical Sciences, 42 (2011) 547-558.
[34] R.S. Singh, G.K. Saini, Pullulan-hyperproducing color variant strain of Aureobasidium pullulans FB-1 newly isolated from phylloplane of Ficus sp, Bioresour Technol, 99 (2008) 3896-3899.
[35] Y. Suginoshita, Y. Tabata, T. Matsumura, Y. Toda, M. Nabeshima, F. Moriyasu, Y. Ikada, T. Chiba, Liver targeting of human interferon-beta with pullulan based on metal coordination, J Control Release, 83 (2002) 75-88.
[36] K. Na, E.S. Lee, Y.H. Bae, Adriamycin loaded pullulan acetate/sulfonamide conjugate nanoparticles responding to tumor pH: pH-dependent cell interaction, internalization and cytotoxicity in vitro, J Control Release, 87 (2003) 3-13.

[37] H. Zhang, F. Li, J. Yi, C. Gu, L. Fan, Y. Qiao, Y. Tao, C. Cheng, H. Wu, Folate-decorated maleilated pullulan-doxorubicin conjugate for active tumor-targeted drug delivery, European journal of pharmaceutical sciences : official journal of the European Federation for Pharmaceutical Sciences, 42 (2011) 517-526.
[38] H. Nogusa, K. Yamamoto, T. Yano, M. Kajiki, H. Hamana, S. Okuno, Distribution characteristics of carboxymethylpullulan-peptide-doxorubicin conjugates in tumor-bearing rats: different sequence of peptide spacers and doxorubicin contents, Biol Pharm Bull, 23 (2000) 621-626.
[39] D. Bruneel, E. Schacht, End group modification of pullulan Polymer, 36 (1995) 169-172.
[40] T.D. Leathers, Biotechnological production and applications of pullulan, Appl Microbiol Biotechnol, 62 (2003) 468-473.
[41] Y. Wang, H. Chen, Y. Liu, J. Wu, P. Zhou, Y. Wang, R. Li, X. Yang, N. Zhang, pH-sensitive pullulan-based nanoparticle carrier of methotrexate and combretastatin A4 for the combination therapy against hepatocellular carcinoma, Biomaterials, 34 (2013) 7181-7190.
[42] S.J. Lee, G.Y. Hong, Y.I. Jeong, M.S. Kang, J.S. Oh, C.E. Song, H.C. Lee, Paclitaxel-incorporated nanoparticles of hydrophobized polysaccharide and their antitumor activity, International journal of pharmaceutics, 433 (2012) 121-128.
[43] P.V. Paranjpe, Y. Chen, V. Kholodovych, W. Welsh, S. Stein, P.J. Sinko, Tumor-targeted bioconjugate based delivery of camptothecin: design, synthesis and in vitro evaluation, Journal of controlled release : official journal of the Controlled Release Society, 100 (2004) 275-292.
[44] Y. Wang, Y. Liu, Y. Liu, W. Zhou, H. Wang, G. Wan, D. Sun, N. Zhang, Y. Wang, A polymeric prodrug of cisplatin based on pullulan for the targeted therapy against hepatocellular carcinoma, International journal of pharmaceutics, 483 (2015) 89-100.
[45] G. Bonzi, S. Salmaso, A. Scomparin, A. Eldar-Boock, R. Satchi-Fainaro, P. Caliceti, Novel pullulan bioconjugate for selective breast cancer bone metastases treatment, Bioconjugate chemistry, 26 (2015) 489-501.
[46] T. Minko, M.L. Patil, M. Zhang, J.J. Khandare, M. Saad, P. Chandna, O. Taratula, LHRH-targeted nanoparticles for cancer therapeutics, Methods Mol Biol, 624 (2010) 281-294.
[47] Q. Xu, Y. Liu, S. Su, W. Li, C. Chen, Y. Wu, Anti-tumor activity of paclitaxel through dual-targeting carrier of cyclic RGD and transferrin conjugated hyperbranched copolymer nanoparticles, Biomaterials, 33 (2012) 1627-1639.
[48] H. Shmeeda, D. Tzemach, L. Mak, A. Gabizon, Her2-targeted pegylated liposomal doxorubicin: retention of target-specific binding and cytotoxicity after in vivo passage, J Control Release, 136 (2009) 155-160.
[49] S. Salmaso, J.S. Pappalardo, R.R. Sawant, T. Musacchio, K. Rockwell, P. Caliceti, V.P. Torchilin, Targeting glioma cells in vitro with ascorbate-conjugated pharmaceutical nanocarriers, Bioconjug Chem, 20 (2009) 2348-2355.
[50] Eldar-Boock A, Polyak D, S.-F. R, Ligand-assisted vascular targeting of polymer therapeutics. , in: S.P. Kratz F (Ed.) Drug Delivery in Oncology – From Basic Research to Cancer Therapy. , Weinheim, Germany: Wiley-VCH Verlag GmbH & Co. KGaA, 2011.
[51] J.M. Shillingford, C.P. Leamon, I.R. Vlahov, T. Weimbs, Folate-conjugated rapamycin slows progression of polycystic kidney disease, Journal of the American Society of Nephrology : JASN, 23 (2012) 1674-1681.
[52] Y. Lu, T.W. Stinnette, E. Westrick, P.J. Klein, M.A. Gehrke, V.A. Cross, I.R. Vlahov, P.S. Low, C.P. Leamon, Treatment of experimental adjuvant arthritis with a novel folate receptor-targeted folic acid-aminopterin conjugate, Arthritis research & therapy, 13 (2011) R56.
[53] A. Gabizon, D. Tzemach, J. Gorin, L. Mak, Y. Amitay, H. Shmeeda, S. Zalipsky, Improved therapeutic activity of folate-targeted liposomal doxorubicin in folate receptor-expressing tumor models, Cancer chemotherapy and pharmacology, 66 (2010) 43-52.

[54] H. Shmeeda, L. Mak, D. Tzemach, P. Astrahan, M. Tarshish, A. Gabizon, Intracellular uptake and intracavitary targeting of folate-conjugated liposomes in a mouse lymphoma model with up-regulated folate receptors, Molecular cancer therapeutics, 5 (2006) 818-824.
[55] A. Gabizon, A.T. Horowitz, D. Goren, D. Tzemach, F. Mandelbaum-Shavit, M.M. Qazen, S. Zalipsky, Targeting folate receptor with folate linked to extremities of poly(ethylene glycol)-grafted liposomes: in vitro studies, Bioconjugate chemistry, 10 (1999) 289-298.
[56] T. Ben-Mordechai, R. Holbova, N. Landa-Rouben, T. Harel-Adar, M.S. Feinberg, I. Abd Elrahman, G. Blum, F.H. Epstein, Z. Silman, S. Cohen, J. Leor, Macrophage subpopulations are essential for infarct repair with and without stem cell therapy, Journal of the American College of Cardiology, 62 (2013) 1890-1901.
[57] A. Gabizon, F. Martin, Polyethylene glycol-coated (pegylated) liposomal doxorubicin. Rationale for use in solid tumours, Drugs, 54 Suppl 4 (1997) 15-21.
[58] L.M. Kaminskas, V.M. McLeod, B.D. Kelly, G. Sberna, B.J. Boyd, M. Williamson, D.J. Owen, C.J. Porter, A comparison of changes to doxorubicin pharmacokinetics, antitumor activity, and toxicity mediated by PEGylated dendrimer and PEGylated liposome drug delivery systems, Nanomedicine, 8 (2012) 103-111.
[59] L.M. Kaminskas, V.M. McLeod, B.D. Kelly, C. Cullinane, G. Sberna, M. Williamson, B.J. Boyd, D.J. Owen, C.J. Porter, Doxorubicin-conjugated PEGylated dendrimers show similar tumoricidal activity but lower systemic toxicity when compared to PEGylated liposome and solution formulations in mouse and rat tumor models, Mol Pharm, 9 (2012) 422-432.
[60] K. Kawano, Y. Maitani, Effects of polyethylene glycol spacer length and ligand density on folate receptor targeting of liposomal Doxorubicin in vitro, Journal of drug delivery, 2011 (2011) 160967.
[61] K. Riviere, Z. Huang, K. Jerger, N. Macaraeg, F.C. Szoka, Jr., Antitumor effect of folate-targeted liposomal doxorubicin in KB tumor-bearing mice after intravenous administration, Journal of drug targeting, 19 (2011) 14-24.
[62] C.P. Leamon, J.A. Reddy, I.R. Vlahov, P.J. Kleindl, M. Vetzel, E. Westrick, Synthesis and biological evaluation of EC140: a novel folate-targeted vinca alkaloid conjugate, Bioconjug Chem, 17 (2006) 1226-1232.
[63] C.P. Leamon, J.A. Reddy, I.R. Vlahov, M. Vetzel, N. Parker, J.S. Nicoson, L.C. Xu, E. Westrick, Synthesis and biological evaluation of EC72: a new folate-targeted chemotherapeutic, Bioconjug Chem, 16 (2005) 803-811.
[64] J.A. Reddy, E. Westrick, I. Vlahov, S.J. Howard, H.K. Santhapuram, C.P. Leamon, Folate receptor specific anti-tumor activity of folate-mitomycin conjugates, Cancer Chemother Pharmacol, 58 (2006) 229-236.
[65] C. Liu, J. Yuan, X. Luo, M. Chen, Z. Chen, Y. Zhao, X. Li, Folate-decorated and reduction-sensitive micelles assembled from amphiphilic polymer-camptothecin conjugates for intracellular drug delivery, Mol Pharm, 11 (2014) 4258-4269.
[66] G.B. Zhang, X.L. Cui, D.L. Sui, X.H. Ren, Z. Zhang, Z.C. Wang, S. Lin, Differential molecular genetic analysis in glioblastoma multiforme of long- and short-term survivors: a clinical study in Chinese patients, J Neurooncol, (2013).
[67] Y. Hattori, J. Yamashita, C. Sakaida, K. Kawano, E. Yonemochi, Evaluation of antitumor effect of zoledronic acid entrapped in folate-linked liposome for targeting to tumor-associated macrophages, Journal of liposome research, (2014) 1-10.
[68] H. Shmeeda, Y. Amitay, D. Tzemach, J. Gorin, A. Gabizon, Liposome encapsulation of zoledronic acid results in major changes in tissue distribution and increase in toxicity, J Control Release, 167 (2013) 265-275.
[69] M. Licciardi, D. Paolino, C. Celia, G. Giammona, G. Cavallaro, M. Fresta, Folate-targeted supramolecular vesicular aggregates based on polyaspartyl-hydrazide copolymers for the selective delivery of antitumoral drugs, Biomaterials, 31 (2010) 7340-7354.
[70] E. Vlashi, L.E. Kelderhouse, J.E. Sturgis, P.S. Low, Effect of folate-targeted nanoparticle size on their rates of penetration into solid tumors, ACS nano, 7 (2013) 8573-8582.

[71] K. Zhang, Q. Wang, Y. Xie, G. Mor, E. Sega, P.S. Low, Y. Huang, Receptor-mediated delivery of siRNAs by tethered nucleic acid base-paired interactions, RNA, 14 (2008) 577-583.
[72] C.R. Patra, R. Bhattacharya, P. Mukherjee, Fabrication and functional characterization of goldnanoconjugates for potential application in ovarian cancer, J Mater Chem, 20 (2010) 547-554.
[73] S.Y. Lin, W.R. Lee, Y.F. Su, S.P. Hsu, H.C. Lin, P.Y. Ho, T.C. Hou, Y.P. Chou, C.T. Kuo, W.S. Lee, Folic acid inhibits endothelial cell proliferation through activating the cSrc/ERK 2/NF-kappaB/p53 pathway mediated by folic acid receptor, Angiogenesis, 15 (2012) 671-683.
[74] X.Q. Pan, H. Wang, R.J. Lee, Antitumor activity of folate receptor-targeted liposomal doxorubicin in a KB oral carcinoma murine xenograft model, Pharmaceutical research, 20 (2003) 417-422.
[75] R.N. Mamidi, S. Weng, S. Stellar, C. Wang, N. Yu, T. Huang, A.P. Tonelli, M.F. Kelley, A. Angiuoli, M.C. Fung, Pharmacokinetics, efficacy and toxicity of different pegylated liposomal doxorubicin formulations in preclinical models: is a conventional bioequivalence approach sufficient to ensure therapeutic equivalence of pegylated liposomal doxorubicin products?, Cancer Chemother Pharmacol, 66 (2010) 1173-1184.
[76] A. De Angelis, E. Piegari, D. Cappetta, L. Marino, A. Filippelli, L. Berrino, J. Ferreira-Martins, H. Zheng, T. Hosoda, M. Rota, K. Urbanek, J. Kajstura, A. Leri, F. Rossi, P. Anversa, Anthracycline cardiomyopathy is mediated by depletion of the cardiac stem cell pool and is rescued by restoration of progenitor cell function, Circulation, 121 (2010) 276-292.
[77] T. Eschenhagen, T. Force, M.S. Ewer, G.W. de Keulenaer, T.M. Suter, S.D. Anker, M. Avkiran, E. de Azambuja, J.L. Balligand, D.L. Brutsaert, G. Condorelli, A. Hansen, S. Heymans, J.A. Hill, E. Hirsch, D. Hilfiker-Kleiner, S. Janssens, S. de Jong, G. Neubauer, B. Pieske, P. Ponikowski, M. Pirmohamed, M. Rauchhaus, D. Sawyer, P.H. Sugden, J. Wojta, F. Zannad, A.M. Shah, Cardiovascular side effects of cancer therapies: a position statement from the Heart Failure Association of the European Society of Cardiology, Eur J Heart Fail, 13 (2011) 1-10.
[78] T. Safra, F. Muggia, S. Jeffers, D.D. Tsao-Wei, S. Groshen, O. Lyass, R. Henderson, G. Berry, A. Gabizon, Pegylated liposomal doxorubicin (doxil): reduced clinical cardiotoxicity in patients reaching or exceeding cumulative doses of 500 mg/m2, Annals of oncology : official journal of the European Society for Medical Oncology / ESMO, 11 (2000) 1029-1033.

Table I: Chemical composition of the pullulan conjugates

	(NH_2-PEG)-Pull-(Cyst-Dox)		(FA-PEG)-Pull-(Cyst-Dox)	
Composition	**(% w/w)**	**(mol %)**	**(% w/w)**	**(mol %)**
Glucose	33.7	53.4	29.1	49.3
Derivatized glucose	14.7	23.4	12.6	21.3
1.9 kDa PEG(NH_2)$_2$	42.3	6.4	40.4	6.5
Cysteamine	5	14.4	4.7	14.5
Doxorubicin	4.3	2.1	6.3	3.4
Folic Acid	-	-	6.9	4.8

Table II: Chemical composition of the liposomal formulations

	PLD		PLD-FA	
Composition	**(mg/mL)**	**(mol%)**	**(mg/mL)**	**(mol%)**
m-PEG-DSPE	3.19	4.56	3.19	4.57
Cholesterol	3.19	32.51	3.19	32.64
HPSC	9.58	50.53	9.58	48.60
Doxorubicin	2	14.46	1.91	13.87
Folic acid	-	-	0.034	0.3

Table III: Physico-chemical characterization of Dox delivery systems

Physico-chemical property	**(NH_2-PEG)-Pull-(Cyst-Dox)**	**(FA-PEG)-Pull-(Cyst-Dox)**	**PLD**	**PLD-FA**
Theoretical Molecular weight	155 kDa	162 kDa	-	-
Hydrodynamic volume	24.3 ± 5.3 nm (3.3%) 144.8 ±65.15 nm (96.7%)	16.6 ± 3 nm (1.5%) 96.8 ±44.6 nm (98.5%)	84.5 nm (*PDI = 0.053)	79.6 nm (*PDI = 0.115)
Zeta potential	-4.94 mV	-5.43 mV	-7.73 mV	- 9.75 mV

* PDI= Polydispersity

Table IV: IC_{50} on KB HiFR cells and on HUVEC

	Long-term exposure (72 h)		Short-term exposure (1 h+72 h)	
IC_{50} / **Compound**	**HiFR-KB (nM)**	**HUVEC (nM)**	**HiFR-KB (nM)**	**HUVEC (nM)**
Dox	0.4	1	50	150
(FA-PEG)-Pull-(Cyst-Dox)	20	20	4000	800
(NH_2-PEG)-Pull-(Cyst-Dox)	2000	400	20000	30000
PLD-FA	200	150	4000	400
PLD	200	300	20000	30000

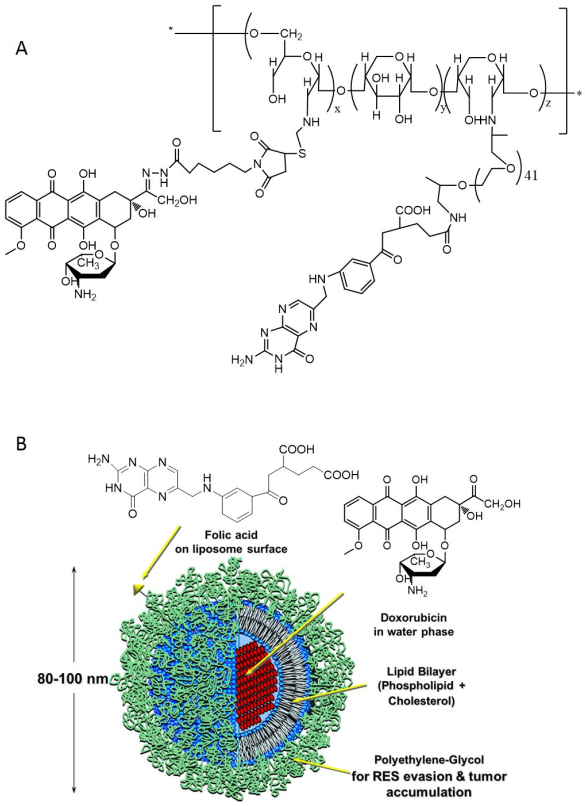

Figure 1 - Chemical structures of (A) (FA-PEG)-Pull-(Cyst-Dox), and (B) PLD-FA.

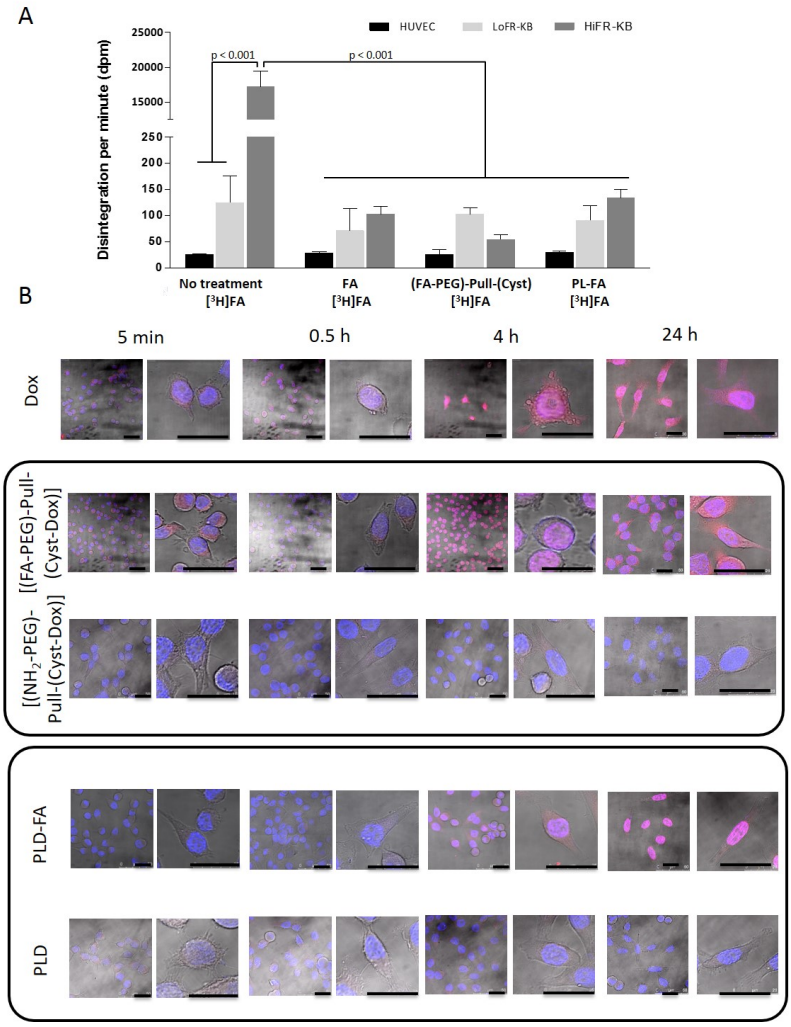

Figure 2 - Folated nanocarriers compete with FA for the internalization to FR-overexpressing cells to which they are rapidly internalized. (A) HUVEC, LoFR-KB and HiFR-KB cells were incubated with 0.2 μM [^{3}H]FA alone or with cold non-radiolabelled FA, (FA-PEG)-Pull-(Cyst) or PL-FA at 2 μM FA-equivalent. [^{3}H]FA is internalized by HiFR-KB cells, while the internalization is negligible in the subline cultured in regular medium, i.e. LoFR-KB cells ($p<10^{-6}$). The intracellular radioactivity dramatically decreases when the HiFR-KB cells are treated with cold FA, (FA-PEG)-Pull-(Cyst) or PL-FA ($p<10^{-9}$) competing on the binding to the FR. HUVEC shows no internalization of the radioactive FA. (B) HiFR-KB cells were incubated with Dox, with (FA-PEG)-Pull-(Cyst-Dox), (NH_2-PEG)-Pull-(Cyst-Dox), PLD-FA or PLD at 200 nM Dox-equivalent in FF-RPMI. The (FA-PEG)-Pull-(Cyst-Dox) conjugated with folic acid is internalized after 5 min, and after 30 min the released Dox is in the nucleus, as colocalization with DAPI occurs. PLD-FA is internalized after 4 h, and the internalization of (NH_2-PEG)-Pull-(Cyst-Dox) and PLD at the same time point is negligible. Scale bar = 25 μm.

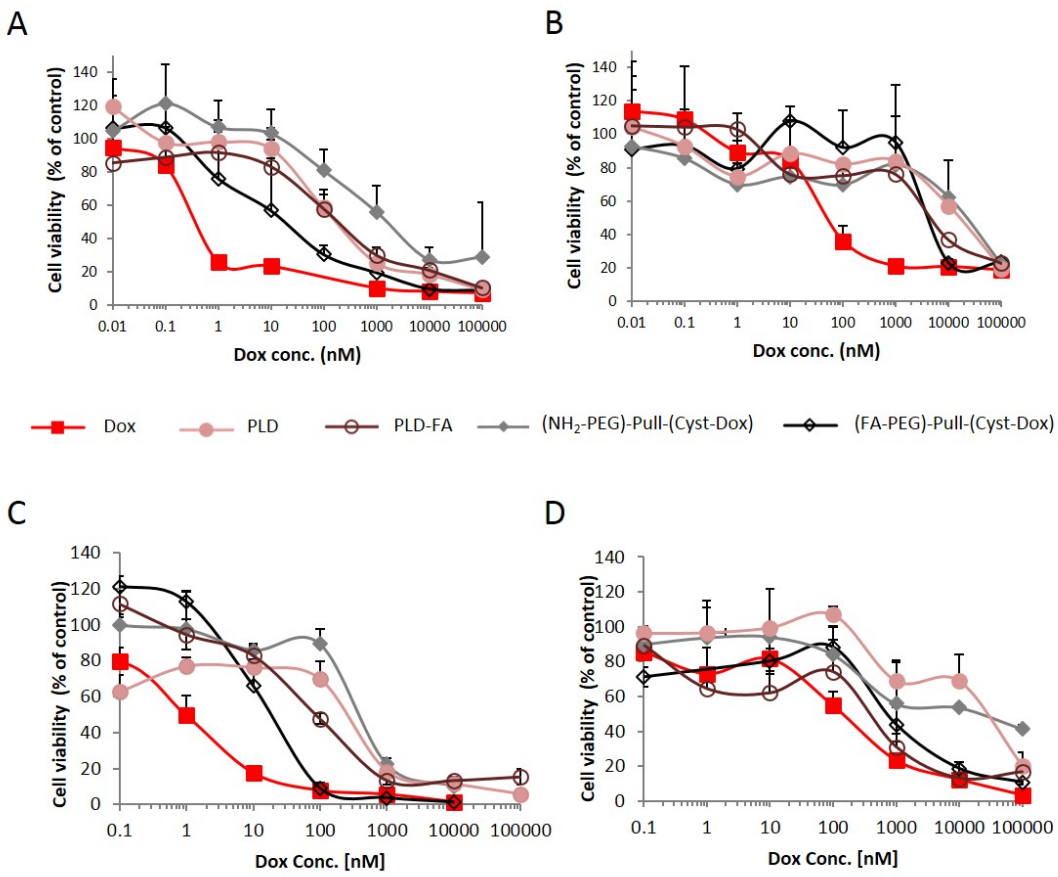

Figure 3 - Folic acid conjugation to nanosystems increase the activity of drug carriers compared with the non-folated ones on HiFR-KB cells and HUVEC treated for prolong and short-term exposure. HiFR-KB cells exposed to a serial dilution of Dox, (FA-PEG)-Pull-(Cyst-Dox), (NH_2-PEG)-Pull-(Cyst-Dox), PLD-FA or PLD for (A) long-term (72 h) (IC_{50} of non-folated pullulan was higher than folated pullulan bioconjugate, $p<10^{-4}$ or for (B) short-term (1+72 h) (IC_{50} of non-folated pullulan was higher than folated pullulan bioconjugate $p<10^{-7}$. Anti-proliferative activity was evaluated incubating **HUVEC** with serial dilutions of Dox, (FA-PEG)-Pull-(Cyst-Dox), (NH_2-PEG)-Pull-(Cyst-Dox), PLD-FA and PLD for (C) Long-term exposure (72 h) (IC_{50} of non-folated pullulan was higher than folated pullulan bioconjugate $p<10^{-14}$, non-folated was higher than folated liposome $p<10^{-5}$) or (D) short-term exposure (1+72 h) (IC_{50} of non-folated was higher than folated pullulan bioconjugate $p<10^{-5}$, non-folated was higher than folated liposome $p<10^{-5}$). Data represents mean ± s.d. X-axis is presented at a logarithmic scale.

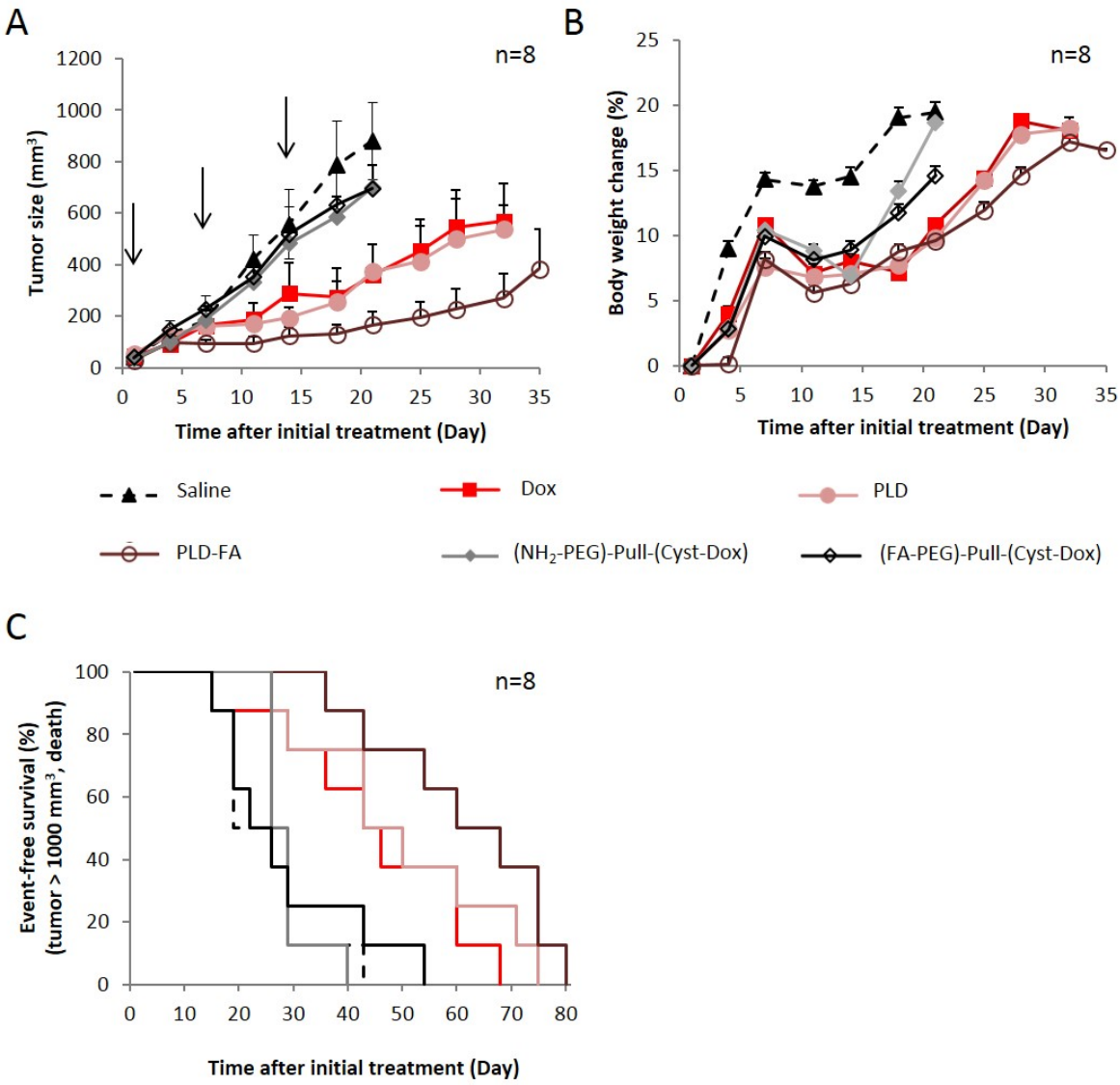

Figure 4 – Three weekly i.v. injections of PLD and PLD-FA maintain and increase the ability of Dox to inhibit KB tumor growth in mice. Mice were treated once a week for three weeks with Dox, (FA-PEG)-Pull-(Cyst-Dox), (NH_2-PEG)-Pull-(Cyst-Dox), PLD-FA or PLD at 5 mg/Kg Dox-equivalent dose. (A) PLD and PLD-FA inhibited tumor growth compared to saline (p= 0.046), (B) did not cause any body weight loss, and (C) prolonged survival compared to saline (Log-rank test p=0.004 for PLD and p=0.0002 for PLD-FA).

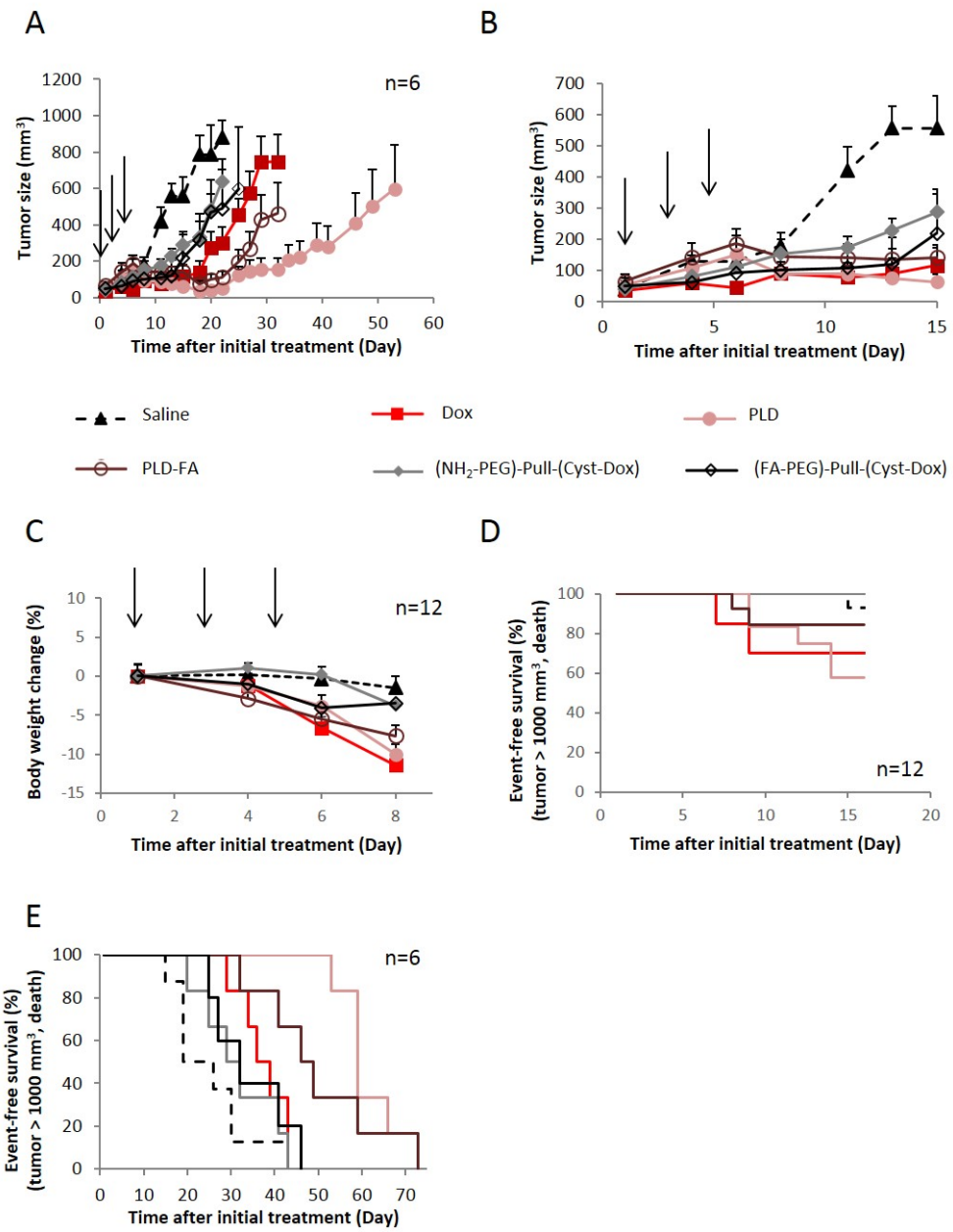

Figure 5 - Three every-other-day i.v. injections of FR-targeted and non-folated polymeric and liposomal formulations maintain and increase the ability of Dox to inhibit KB tumor growth in mice. Mice were treated three times in 6 days with 5 mg/Kg Dox-equivalent dose of Dox, (FA-PEG)-Pull-(Cyst-Dox), (NH_2-PEG)-Pull-(Cyst-Dox), PLD-FA or PLD. (A) All formulations inhibited tumor growth while only PLD was significant compared to saline throughout the study, $p<10^{-9}$. Dox, PLD-FA, folated and non-folated pullulan bioconjugates significantly inhibited tumor growth by 65%, 87%, 40% and 40%, respectively, till day 20. (B) Enlargement of graph in panel A (First 15 days of the experiment). (C) Pullulan bioconjugates did not cause body weight loss while liposomal formulations did, however reversible following treatment discontinuation. (D) Survival of mice treated with Dox, PLD and PLD was affected by toxic death during treatment, but (E) the overall survival following treatment discontinuation was prolonged compared to saline (Log-rank test: Dox $p=0.05$, PLD $p=0.0005$ and PLD-FA $p=0.0046$).

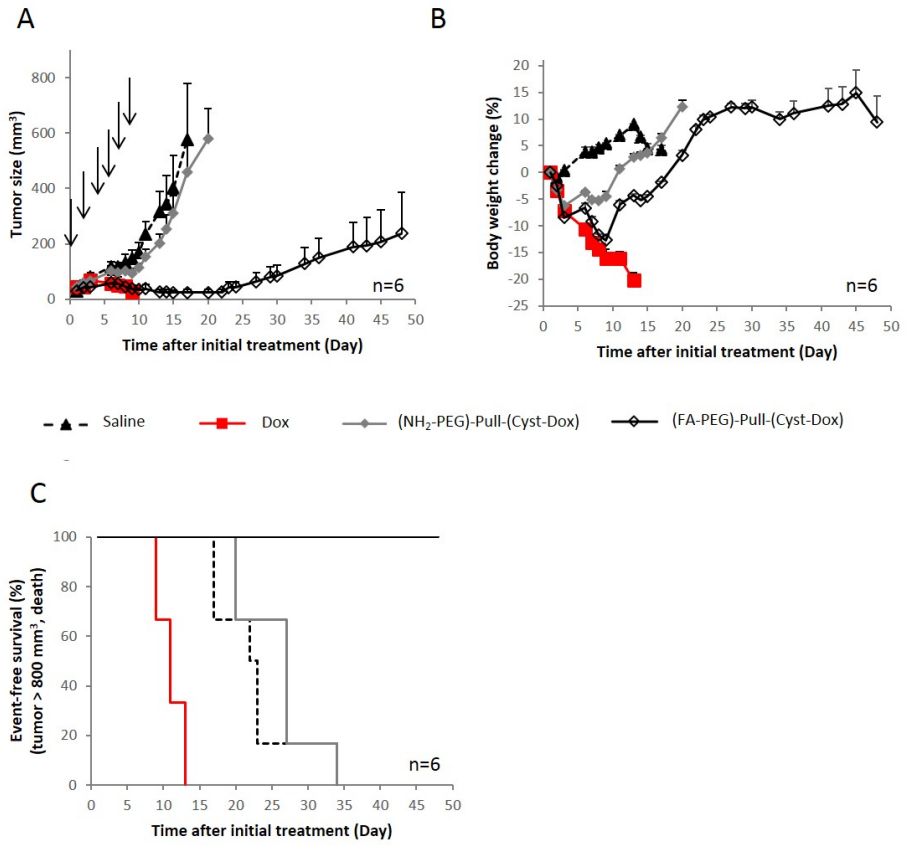

Figure 6 – Six i.v. injections of (FA-PEG)-Pull-(Cyst-Dox) significantly inhibit KB tumor growth. Mice were treated six times with 5 mg/Kg of Dox or Dox-equivalent dose of (FA-PEG)-Pull-(Cyst-Dox), (NH_2-PEG)-Pull-(Cyst-Dox), PLD-FA or PLD. (A) (FA-PEG)-Pull-(Cyst-Dox) reduced tumor size by 96% compared to saline on day 19 ($p<10^{-12}$), (B) causing reversible moderate body weight loss, and (C) extending survival up to 50 days after the first treatment (Log-rank test: p=0.0014).

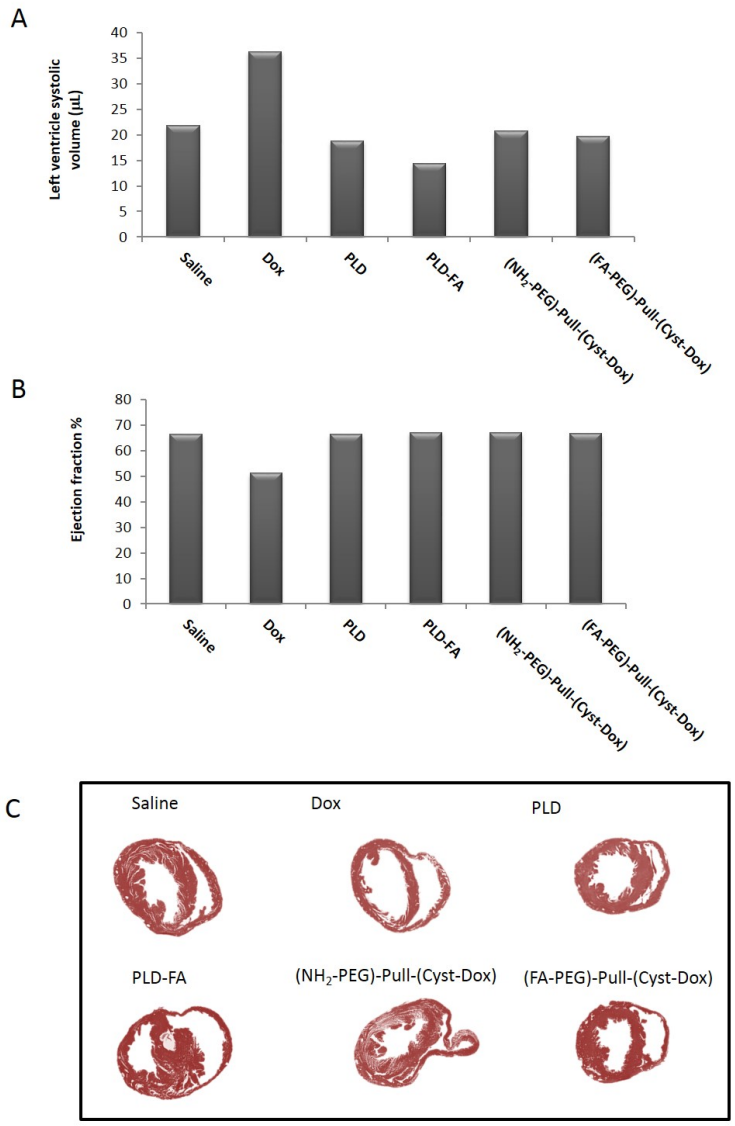

Figure 7 – FR-targeted and non-folated polymeric and liposomal formulations reduce Dox-induced cardiotoxicity in mice. Mice treated with Dox showed impaired functionality displaying (A) greatest left ventricle systolic volume and (B) lowest LV ejection fraction ten days following treatment discontinuation. (C) Histological staining with Masson-Trichrome of hearts of mice treated three times in 6 days with saline or 5 mg/Kg of Dox or Dox-equivalent dose of PLD-FA, PLD, (FA-PEG)-Pull-(Cyst-Dox), or (NH_2-PEG)-Pull-(Cyst-Dox).